*Annals of Work Exposures and Health*, 2022, Vol. 66, No. 5, 656–670
https://doi.org/10.1093/annweh/wxab076
Advance Access publication 5 October 2021
Original Article



Original Article

# Aerosol Analysis Using Handheld Raman Spectrometer: On-site Quantification of Trace Crystalline Silica in Workplace Atmospheres

**Shijun Wei[1,2], Belinda Johnson[1], Michael Breitenstein[1], Lina Zheng[1,3], John Snawder[1] and Pramod Kulkarni[1,*]**

[1]Centers for Disease Control and Prevention, National Institute for Occupational Safety and Health, Cincinnati, OH 45226, USA; [2]Department of Mechanical and Materials Engineering, University of Cincinnati, Cincinnati, OH 45221, USA [3]Present address: Department of Industrial Hygiene Engineering, School of Safety Engineering, China University of Mining and Technology, Xuzhou 221116, Jiangsu, P.R. China.

*Author to whom correspondence should be addressed. Tel: +1-513-841-4300; fax: +1-513-841-4545; e-mail: PSKulkarni@cdc.gov

Submitted 1 February 2021; revised 11 August 2021; editorial decision 22 August 2021; revised version accepted 30 August 2021.

## Abstract

A method for aerosol chemical analysis using handheld Raman spectrometer has been developed and its application to measurement of crystalline silica concentration in workplace atmosphere is described. The approach involves collecting aerosol as a spot sample using a wearable optical aerosol monitor, followed by direct-on-filter quantitative analysis of the spot sample for crystalline silica using handheld Raman spectrometer. The filter cassette of a commercially available optical aerosol monitor (designed to collect aerosol for post-shift analysis) was modified to collect 1.5-mm-diameter spot sample, which provided adequate detection limits for short-term measurements over a few tens of minutes or hours. The method was calibrated using aerosolized $\alpha$-quartz standard reference material in the laboratory. Two Raman spectrometers were evaluated, one a handheld unit (weighing less than 410 g) and the other a larger probe-based field-portable unit (weighing about 5 kg). The lowest limit of quantification for $\alpha$-quartz of 16.6 $\mu$g m$^{-3}$ was obtained using the handheld Raman unit at a sample collection time of 1 h at 0.4 l min$^{-1}$. Short-term measurement capability and sensitivity of the Raman method were demonstrated using a transient simulated workplace aerosol. Workplace air and personal breathing zone concentrations of crystalline silica of workers at a hydraulic fracturing worksite were measured using the Raman method. The measurements showed good agreement with the co-located samples analyzed using the standard X-ray powder diffraction (XRD) method, agreeing within 0.15–23.2% of each other. This magnitude of difference was comparable to the inter- and intra-laboratory analytical precision of established XRD and infrared methods. The pilot study shows that for silica-containing materials studied in this work it is possible to obtain quantitative measurements with good analytical figures of merit using handheld or portable Raman

**What's Important About This Paper?**

This manuscript describes development of a new method for rapid, on-site exposure measurement of respirable crystalline silica (RCS) aerosols in workplace atmospheres. The method provides short-term measurements with good precision and accuracy at detection limits that are an order of magnitude lower than current standard methods. This method has broad applicability to other environmental and occupational aerosols. The study is timely and makes critical contribution to RCS exposure assessment and aerosol analytical methods in general.

spectrometers. Further studies will be needed to assess matrix interferences and measurement uncertainty for several other types of particle matrices to assess the broader applicability of the method.

**Keywords:** crystalline silica aerosol; Raman spectroscopy; infrared spectroscopy

## Introduction

Respirable crystalline silica (RCS) is generated by various industrial and construction activities such as cutting, grinding, and sawing of industrial materials such as stone, composites, bricks, and concretes (Chisholm, 1999; Akbar-Khanzadeh and Brillhart, 2002; Baron *et al.*, 2002; Linch, 2002; Rappaport *et al.*, 2003; Yassin *et al.*, 2005; Meeker *et al.*, 2009; Esswein *et al.*, 2013; OSHA, 2016). Exposure to RCS from such activities affects about 2.3 million workers across 600 000 workplaces in the USA (OSHA, 2016). Long-term exposure to crystalline silica leads to silicosis, lung cancer, and chronic obstructive pulmonary disease (COPD) (NIOSH, 1987). International Agency for Research on Cancer (IARC) has recognized RCS as a Group 1 human carcinogen (IARC, 1997, 2012). In 2010, the American Conference of Governmental Industrial Hygienists (ACGIH) (ACGIH, 2006) recommended a lower standard of 25 μg $m^{-3}$. In 2016, the Occupational Safety and Health Administration (OSHA) reduced the permissible exposure limit (PEL) from 100 μg $m^{-3}$ to 50 μg $m^{-3}$ (8-h time-weighted average) (OSHA, 2016).

The current standard methods for estimating RCS in workplace air, such as the NIOSH method 7603 (NIOSH, 2017) using infrared absorption spectrometry (IR) and NIOSH method 7500 (NIOSH, 2003) using X-ray powder diffraction (XRD), were developed for 8-h sample collection. These methods are not suitable for on-site or direct-reading analysis as they require sample pretreatment and laboratory analysis. There is a need for rapid, on-site quantification methods to improve air monitoring in workplace atmospheres needed to reduce occupational exposures to crystalline silica.

New analytical methods with lower detection limits have been recently developed using quantum cascade laser-based infrared absorption spectroscopy (Wei *et al.*, 2017; Wei *et al.*, 2020) and Raman spectroscopy (Stacey *et al.*, 2017; Zheng *et al.*, 2018). Stacey *et al.* used a research-grade confocal Raman microscope to analyze 25-mm-diameter filters for crystalline silica. Their approach involved redepositing analyte suspension over a 5-mm-diameter spot on silver membrane filters, followed by point analysis of several spots on the filter. They reported limits of quantification (LOQ) between 0.066 and 0.161 μg (Stacey *et al.*, 2017). Recently, Stacey *et al.* (2020) extended the indirect method by using their miniature sampler with 13-mm polyvinyl chloride (PVC) filters, followed by ashing and redepositing on silver membrane filters. They (Stacey *et al.*, 2020) reported a limit of detection (LOD) of 0.26 μg. Zhang *et al.* (Zheng *et al.*, 2018) reported LOD between 8 and 55 ng, using spot aerosol collection techniques and probe-based Raman system. These analytical methods require either research-grade instrumentation or special sample preparation or collection techniques to achieve lower detection limits, which prohibits their use for rapid, direct-reading measurement on-site or in the field. Such direct-reading quantification capability is often useful to promote effective hazard identification, and risk assessment and mitigation.

The objective of this pilot study was to investigate the analytical figures of merit of the direct-on-filter method using the handheld and portable Raman spectrometers. This approach combines the real-time aerosol sensing of the total dust concentration with the post-collection measurement of RCS content on site.

## Experimental methods

### Measurement approach

The measurement scheme used in this work is described in Fig. 1. The overall scheme involves collection of workplace

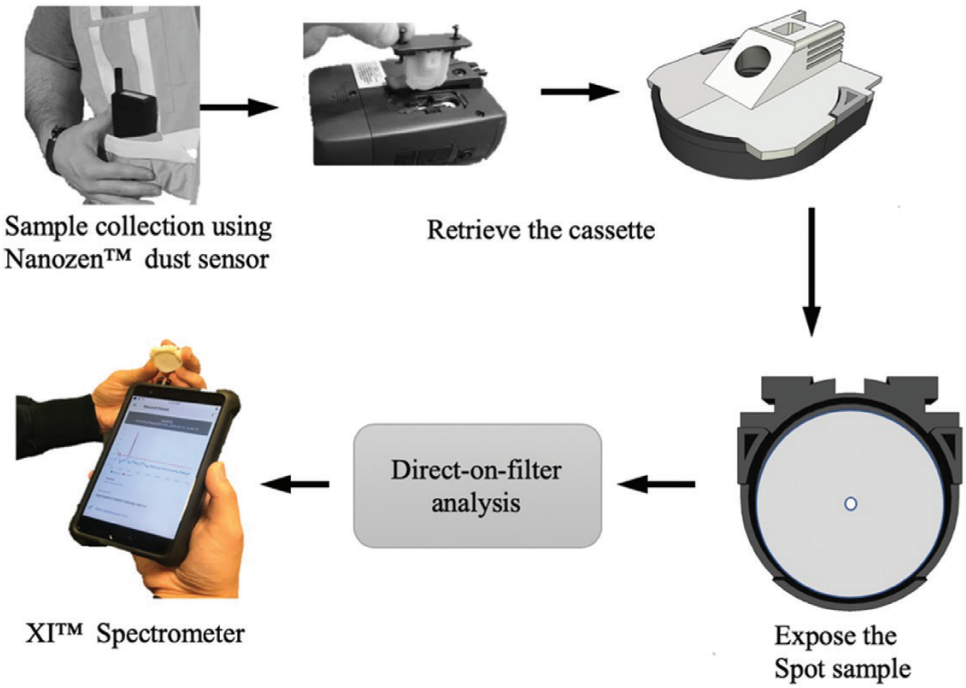


**Figure 1.** A schematic diagram of the sample collection and Raman measurement approach.

aerosols as a spot sample using a wearable Nanozen™ DustCount personal particulate monitor (Series 8899, Nanozen Industries Inc., BC, Canada), retrieval of the filter sample from the Nanozen™ after a predetermined sample collection time, followed by direct-on-filter RCS analysis using a handheld Raman spectrometer.

The Nanozen™ DustCount monitor was used in this study to collect the aerosol as a spot sample with a diameter of 1.5 mm. The monitor is a wearable optical aerosol instrument that measures real-time total mass concentration, particle number concentration, and size distribution of the aerosol. The instrument specifications state that the inlet is a respirable cyclone. There are no published experimental data that show that the inlet cyclone of Nanozen™ meets the International Standards Organization (ISO) respirable convention. The monitor has 20 particle size channels from 0.5 to 10 μm and dynamic range of mass measurement from 1 μg $m^{-3}$ to 21.5 mg $m^{-3}$. The measurement represents the total dust mass concentration, inferred from scattered light from particles, and is not chemically selective to RCS. The monitor also has a built-in removable cassette that allows collection of the sampled aerosol on a 25-mm diameter particulate filter. The filter can be sent to an analytical laboratory for gravimetric analysis or for selective RCS quantification using standard analytical methods (e.g. NIOSH methods 7500 or 7602). The total aerosol concentration can be measured in real-time; however, real-time RCS concentration is not available. The built-in cassette collects the aerosol sample over the entire filter surface. Our earlier work has shown that detection limits of laser spectroscopic techniques can be significantly reduced by collecting aerosol as a spot sample (Wei *et al.*, 2017; Zheng *et al.*, 2018). To obtain a spot sample, we modified the built-in cassette to achieve a spot sample diameter of approximately 1.5 mm. Cassettes with other orifice diameters of 1 mm and 3 mm were also designed and tested. The diameter of 1.5 mm provided a good tradeoff between sensitivity, dynamic range for short-term measurement, and the pressure drop requirements of the Nanozen™ monitor. The modified cassette housed a removable standard 25 mm silver membrane filter (0.8 μm pore size, SKC Inc.). The modified 1.5-mm cassette provided a stable sampling flow rate over the entire shift for particulate mass loadings studied in this work (as verified by the real-time flow rate data retrieved from the instrument post-collection). The filter samples were collected onto the filters directly from the aerosol phase at a flow rate of 0.4 l $min^{-1}$. As noted elsewhere, the silver membrane provides surface enhancement and leads to improved Raman signal (Zheng *et al.*, 2018).

The spot sample was analyzed using a handheld Raman spectrometer (Model XI™; CloudMinds

Technology, Santa Clara, CA, USA). This compact instrument measures 159 × 78.9 × 27 mm and weighs 410 g, allowing convenient handheld measurements in the field. The instrument can be controlled via a touchscreen interface; the measured spectra are immediately displayed on the screen. The compact size allows handheld measurement of filter samples. The excitation laser is delivered through an optical window of the spectrometer, which directly irradiates the sample located at distance of 1.1 cm from the optical lens. A custom adapter was designed that allowed placement of the filter sample at the focal distance of the excitation laser. Supplementary Fig. A1a shows the holder/adapter required for measurement using XI™. The user is required to retrieve the filter cassette from the Nanozen™, attach the adapter to the XI™, and then place the filter sample on the adapter to conduct the Raman analysis. XI™ spectrometer has adjustable output laser power ranging from 100 to 500 mW. Collection times ranging from 3 to 120 s were used in this study. Using high integration time can allow lower detection limit; however at a reduced signal-to-noise ratio.

Additionally, a field-portable, probe-based Raman spectrometer (Model i-Raman; B&W Tek, Newark, DE, USA) was also used to evaluate its performance. This field-portable instrument measures approximately 17 × 34 × 23.4 cm and weighs approximately 3 kg. The i-Raman instrument is transportable by hand to the workplace and can allow on-site measurement. A custom holder was designed to house the Nanozen™ filter cassette and to interface with the i-Raman® probe for direct-on-filter measurement. Supplementary Fig. A1b shows the holder/adapter designed for measurement using i-Raman®. Key specifications and operating characteristics of the two Raman instruments are shown in Table 1.

A typical measurement procedure, using this approach, involved the following steps: (i) sample collection using the Nanozen™ with a modified cassette over a predetermined time, (ii) removal of filter cassette from the Nanozen™, (iii) detaching the top half of the cassette to expose the filter, (iv) placing the bottom half of the cassette (containing the filter) in the custom adapter/holder described above, (v) attaching the Raman spectrometer probe to the adapter/holder, (vi) acquiring the Raman spectrum according to predetermined spectrometer settings (discussed below), and (vii) conducting the spectral analysis and RCS quantification using a predetermined calibration curve. For each sample, three to six repeat measurements were conducted at the same sample location and were averaged. For each particulate mass loading level on the filter, three replicate samples were collected and then averaged.

**Table 1.** The technical specifications of two Raman spectrometers.

| | XI™ | i-Raman® |
|---|---|---|
| Laser wavelength | 785 nm | 785 nm |
| Laser nominal power | 500 mW | 420 mW |
| Laser power at the sample | 380 mW[a] | 320 mW |
| Laser beam diameter at sample[b] | 1000 µm | 2100 µm |
| Wavenumber range | 200–1800 $cm^{-1}$ | 150–3200 $cm^{-1}$ |
| Wavenumber resolution | 8–11 $cm^{-1}$ | 3.5 $cm^{-1}$ |
| Optical interface | Free space | Fiber optic probe |

[a]Estimated value.
[b]Crude estimate obtained using photosensitive liquid crystal cards.

## Calibration methods

The schematic diagram of the experimental setup used for generating calibration curve is shown in Supplementary Fig. A1. Calibration aerosol was generated by aerosolizing aqueous suspensions using a Collison nebulizer (BGI, Butler, NJ, USA), and subsequently passed through a diffusion dryer (TSI Inc., Shoreview, MN, USA) to obtain a dry calibration aerosol. The suspensions containing α-quartz standard reference material (SRM; NIST SRM 1878a) were prepared in ultrafiltered deionized water (CAS 7732-18-5, Thermofisher Scientific, Rochester, NY, USA).

The total particulate mass loading on the collection filters was determined from the measured aerosol mass concentration at the inlet of the collection device, the sample flow rate, and the collection time. The mass concentration of the aerosol was also simultaneously measured using an optical photometer DustTrak™ (Model 8533, TSI Inc.) as shown in Supplementary Fig. A1. The DustTrak™ was gravimetrically calibrated using the SRM. The filter samples from Nanozen™ monitor were then retrieved and were measured by the two portable Raman instruments.

The characteristic peak of α-quartz at a Raman shift frequency of 465 $cm^{-1}$ was used for quantification. For each filter sample, Raman spectra were measured six times at one location (at the centre of the filter) and the mean signal intensity for each sample was obtained by averaging over these six measurements. Calibration curves were constructed by plotting the Raman signal intensity as function of the silica mass loading on the filter. The linear parts of the calibration curves were employed for calculating the sample mass loading below 20 µg, while the nonlinear curve was used for mass loading above 20 µg for both the Raman spectrometers.

LOD ($m_{lod}$) was determined using the 3-σ criteria defined by the International Union of Pure and Applied Chemistry (IUPAC) (Boumans, 1994),

$$m_{lod} = 3\sigma/S_m \quad (1)$$

where σ is the standard deviation of Raman signal of blank filters (that contained no analyte) in the spectral region 400–500 $cm^{-1}$; $S_m$ is the mass measurement sensitivity obtained from the slope of the calibration curve. Three blank filters were used to obtain $3\sigma$. Average spectra for each blank filter was obtained by taking an average over six spectra, following the procedure identical to that used for analyte sample analysis.

### Laboratory test aerosol

Laboratory test aerosol, with the particulate matrix representative of workplace aerosol, were used to evaluate the measurement method. Fine powder, containing particles produced during cutting of engineered stone countertop (ESC), was aerosolized to generate the test aerosol. The ESC fine powder was obtained from the settled dust at an industrial stone countertop fabrication facility, described in detail by Qi and Echt (2019) during grinding and cutting of a thick ESC using a power tool. This ESC material in bulk solid form contained approximately 90% α-quartz according to the ESC manufacturer. Qi and Echt (2019) reported the fractional silica content of the aerosolized RCS at this worksite to be in the range of 12–76%, much lower than the content in the solid bulk form. The remaining particulate matrix contained resins, polymers, and pigments. As shown in Supplementary Fig. A2, filter samples loaded with ESC aerosol were collected at eight different levels of mass loading for Raman measurement and two levels of mass loading for the XRD measurement. For each Raman and XRD measurement, three replicate samples were collected for a given mass loading. The samples were collected on 25-mm silver membrane filters for Raman analysis and on MCE filters for XRD analysis in the laboratory study.

### XRD analysis using NIOSH method 7500

XRD analysis of aerosol samples was performed according to the NIOSH method 7500 (NIOSH, 2003). The analysis was performed by an external laboratory, that did not participate in the Raman study. The Raman measurements were conducted prior to the XRD analysis, and the XRD analyst did not know the expected range or concentration levels of crystalline silica.

As noted earlier, samples for XRD analysis were collected on MCE filters (in laboratory studies) and PVC filters (in field studies). For the standard XRD analysis of the PVC filters (according to the NIOSH method 7500), the filters were first dissolved by tetrahydrofuran (THF). The resulting sample suspension was redeposited on silver membrane filters. The silver-membrane filter was transferred to a sample plate and placed in the automated sample changer for analysis by an X-ray diffractometer (Model# D8 Endeavor with Lynxeye detector; Bruker Corp.). The sample recovery determined using filters spiked with reference quartz material met laboratory quality assurance requirements. The average recovery for quartz was 103%. The relative percent difference result for the duplicate also met the quality assurance requirements. The sample results were not recovery corrected. The limit of quantification for α-quartz for XRD analysis of samples on PVC filter was 17 µg, with an analytical range of 5-2000 µg.

The MCE filters used in XRD analysis were digested using the nitric acid. The average recovery for quartz was 105%. The sample results were not corrected to account for recovery. The limit of quantification for α-quartz for MCE filter analysis was 10 µg, with an analytical range of 3–160 µg.

### Field exposure measurements

Personal breathing zone (PBZ) and area samples were collected at an oil and gas extraction site during hydraulic fracturing operations. The site was representative of hydraulic fracturing where containerized sand is used. The primary source of worker exposure to respirable dust and crystalline silica at this workplace was from handling and transporting large quantities of sand used in subsurface injection and fracturing of rock formations. The sand was transported from the 'sand containers' and dropped into the blender hopper. Sampling was conducted for four consecutive days. For each aerosol sample collected by the Nanozen™ for Raman analysis, a co-located sample was collected for analysis by the standard XRD method.

### Sample collection for standard XRD analysis

PBZ and area samples were collected for respirable dust and crystalline silica measurements and analyzed using the standard XRD method. Sampling flow for each sampling train (SKC XR 5000™ pump, Tygon® tubing, filter cassette, and inlet cyclone) was set and verified in-line before and after sampling event using the air calibrators (BIOS Dry Cal® Defender 520, Mesa Laboratories, Inc.). Samples were collected on pre-weighed PVC filter (5 µm pore size) inside a three-piece sampling cassette (37 mm, polystyrene), fitted with a cyclone inlet (BGI model GK2.69). The

sampling trains were set at a flow rate of 4.2 l $min^{-1}$. Conductive sampling cassettes and cyclones were located in the worker's PBZ by attachment to the lapel/collar of the worker's fire-retardant coveralls. Area air samples were collected from stationary locations close to worker activity (e.g. around sand containers, equipment control stations, cross- and down-wind from emission sources). Samples were collected for the entire working shift. Samples were analyzed in the laboratory gravimetrically to obtain total particulate mass according to the NIOSH method 0600 (NIOSH, 1994) and crystalline silica content according to the NIOSH method 7500 (NIOSH, 2003).

### Sample collection for Raman analysis

Prior to sampling, Nanozen™ monitors were prepared according to manufacturer instructions. Briefly, the impactor of the Nanozen™ was cleaned, oiled, and installed along with supplied conductive tubing on the monitor. Each day a new modified filter cassette with a removable standard 25 mm silver membrane filter (0.8 µm pore size, SKC Inc.) was installed in the monitor. The monitor was turned on and allowed to warm-up for approximately thirty minutes to ensure no leakage and flow stability. To collect PBZ samples, the Nanozen™ was placed on the worker's vest and the inlet of the conductive tubing was attached to its lapel/collar, right next to the inlet of the filter cassette train (used for sample collection for XRD analysis as described above). This ensured that both the Nanozen™ and the filter cassette train sampled the same bolus of air within the worker's PBZ.

Nanozen™ monitors used for area sample collection were co-located with the filter cassette train used for area sample collection for XRD analysis. Monitors remained in place for the entire working shift (8 h). After sampling, the cassettes were removed and placed in individual antistatic bags for transportation to laboratory for Raman analysis. We note that the filter cassettes were not analyzed immediately post-collection in the field due to logistical reasons, though they could be readily analyzed. It was more convenient for the investigators to ship the samples to the laboratory for analysis due to the large number of samples collected in this and a separate but concurrent exposure assessment study.

## Results and discussion

Figure 2a,b show Raman spectra obtained from i-Raman® and XI™ spectrometers for various calibration filter samples with known deposited mass of the SRM ranging from 0.5 to 20.2 µg. Three replicate samples were collected in parallel using three Nanozen™ monitors (see Supplementary Fig. A1). The flow rate, aerosol concentration, and the collection time for all three Nanozen™ sensors were identical. Each filter sample was measured using both the Raman spectrometers after collection. The peak Raman shift frequency at 465 $cm^{-1}$ is from the Si-O-Si symmetric stretching-bending modes (Kingma and Hemley, 1994; Stacey *et al.*, 2017; Zheng *et al.*, 2018; Stacey *et al.*, 2020). Calibration curves were generated using this peak shift frequency. Raman signal was integrated for 30 s for i-Raman® and 60 s for XI™ spectrometer. As expected, the increase in peak height clearly correlates linearly with the particulate mass irradiated by the Raman excitation laser up to a certain mass loading.

Figure 2c,d shows electron micrographs of spot samples at low magnification obtained from the modified Nanozen™ cassettes for low and high particulate mass loadings. At this magnification, the diameter of the deposit was approximately 1.5 mm in diameter. Though the image with 4.3- µg mass loading shows sparsely distributed particulate matter, the high magnification image shows several particles in the centre of the spot where the Raman excitation laser is incident.

The calibration curves were constructed by plotting the peak height, after baseline correction, as a function of the corresponding crystalline silica mass on the filter and are shown in Fig. 3. A baseline was drawn between the Raman shift frequencies at 452 $cm^{-1}$ and 483 $cm^{-1}$. The baseline intensity at 465 $cm^{-1}$ was then subtracted from the peak at 465 $cm^{-1}$ to obtain the peak height corresponding to the Raman signal proportion to RCS content. The vertical error bar around each data point in Fig. 3 represents the standard deviation around the mean obtained by averaging over three replicate measurements. The relative standard deviation (RSD) ranges from 0.4% to 3.6% for XI™ and from 1.2 to 2.9% for i-Raman®, both indicating good repeatability precision. The calibration curves for XI™ at different Raman signal integration times, ranging from 3 to 120 s, are shown in Fig. 3a for mass loading below 20 µg.

Fig. 3b shows calibration curves obtained by normalizing the Raman signal intensity (I; from Fig. 3a) with the corresponding integration time (t) for both spectrometers. The calibration curve is nonlinear at mass loadings above 20 µg. For mass loadings below 20 µg a linear calibration curve is used (best fit for i-Raman® is $I/t = 6.7\ m_p$; best fit for XI™ is $I/t = 54.4\ m_p$—4.1; $R^2 = 0.99$ for both fits). The relative uncertainty of the slope of the linear best fit in Fig. 3b was <<1% for i-Raman® and 1.4% for XI™, respectively. Since Raman signal intensity is proportional to time (Fig. 3a), these

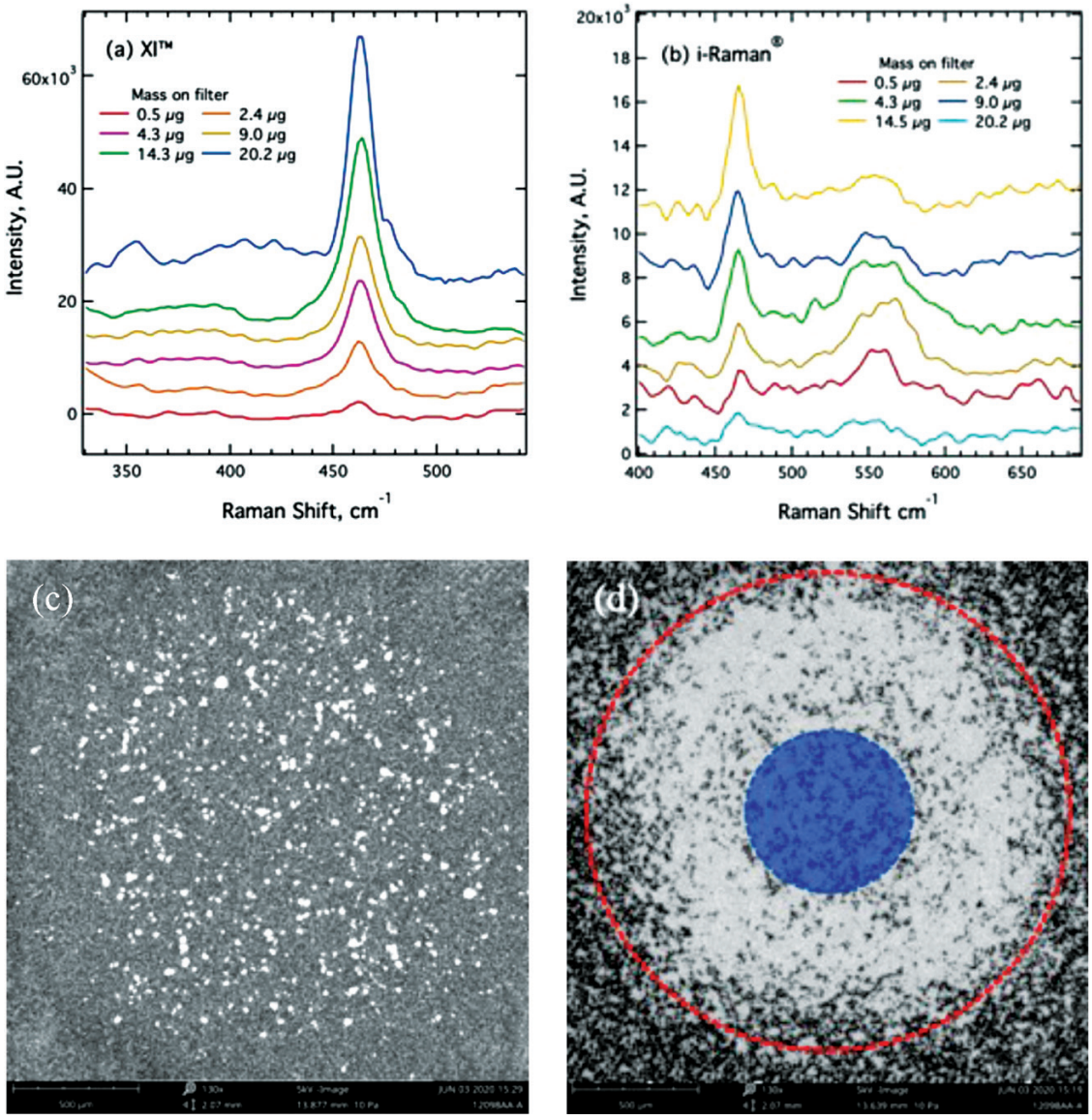


**Figure 2.** Raman spectra of RCS collected on silver membrane filter obtained using (a) XI™ and (b) i-Raman®. The mass loading shown is the mass of RCS on the silver membrane filter estimated using an optical photometer DustTrak™ at a collection time of 30 min. The lowest mass loading of 0.5 μg is at limit of quantification of XI™ and below that of i-Raman®. Also shown are electron micrographs of spot sample obtained from the modified Nanozen™ filter cassettes for particulate mass of: (c) 4.3 μg; (d) 20.2 μg. The blue region in the center corresponds to the crude estimate of laser spot incident on the sample.

calibrations curves allow their application to spectra acquired with an arbitrary integration time and eliminate the need to fix the signal integration time *a priori*.

Nonlinearity at high mass loadings was attributed to increasing thickness of the spot sample, which leads to disproportionate increase in analyte mass irradiated by the Raman excitation laser, until the signal saturates at a certain deposit thickness beyond which there is no increase. For XI™, the nonlinear portion of the curve up to 80 μg appears to provide acceptable uncertainty; however, with the i-Raman® spectrometer mass loadings above 35 μg will likely yield poor uncertainty.

The mass of analyte ($m$) in Fig. 3 (shown on x-axis) was obtained using the aerosol concentration (of the SRM) measured by DustTrak™ ($C_{total}$), the aerosol flow rate ($Q$), and the collection time ($t$). RSD of aerosol sampling flowrate of Nanozen™ was estimated from

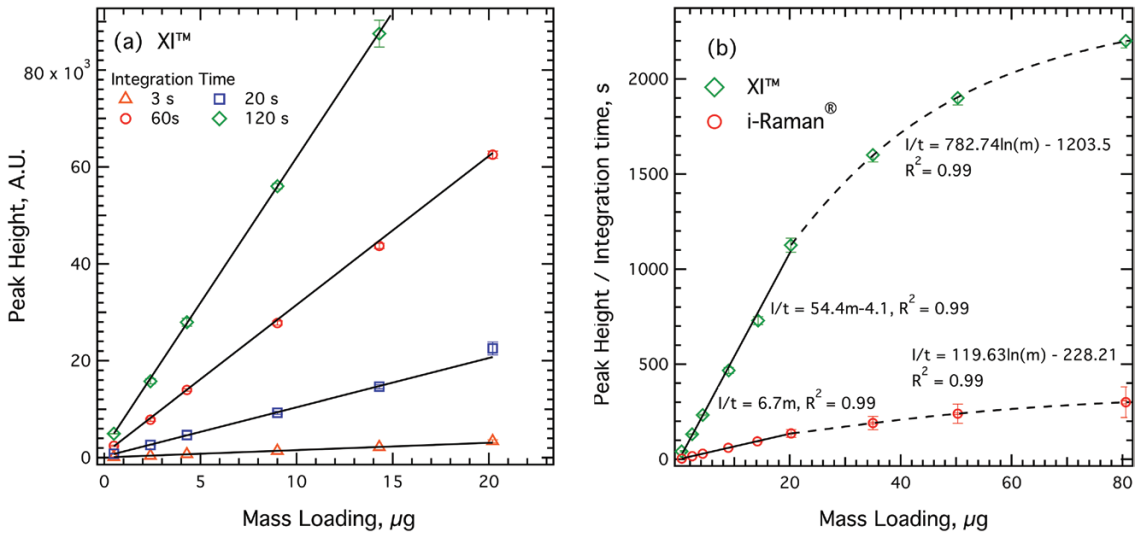


**Figure 3.** (a) Calibration curves obtained for the samples collected with the Nanozen™ device using XI™ signal intensity for four different integration times, and (b) Universal calibration curve for both Raman spectrometers developed by plotting theRamansignal intensity per unit integration time as a function of mass loading on filter.A nonlinear curve is used for loadings beyond 20 μg.

our laboratory measurements to be between 2.4 and 3.2% (the reported uncertainty from the manufacturer is <5%). Overall, relative uncertainty of DustTrak™ for measurement of aerosol concentration, deduced from the standard error of mean concentration measured over the largest time period used in this study, was in the range of 8–13%. The relative uncertainty associated with mass measurement, obtained through propagation of uncertainties (Chen *et al.*, 2011) using the equation, $m = C_{total}.Q.t$, was estimated to be in the range of 6–13%. The horizontal error bars, that represent standard deviation around the mean measured mass, were calculated for the data points in Fig. 3; however, the values are too small to be seen.

The sensitivity of the XI™ spectrometer is approximately four times greater than that of the i-Raman® (slope of the linear calibration curve in Fig. 3). This is likely due to higher optical throughput of the XI™ (due to combination of slit width and free-space optical coupling with the sample) at the expense of lower spectral resolution (Mu *et al.*, 2019). The LODs were determined to be 0.12 and 0.46 μg for XI™ and i-Raman®, respectively and are shown in Table 2. Assuming the sample collection time of 60 min, the corresponding LODs in terms of air concentration are 5 μg m$^{-3}$ and 17.25 μg m$^{-3}$ XI™ and i-Raman®, respectively. These detection limits are significantly lower compared to that of the standard XRD method used in this study (~3–6 μg) and can allow short-term as well as full-shift measurement below the new permissible exposure limits.

**Table 2.** Crystalline silica detection limits of two portable Raman spectrometers.

| | Limit of detection | |
|---|---|---|
| | Mass, μg | Air concentration[a], μg m$^{-3}$ |
| i-Raman® spectrometer | 0.46 | 17.25[a] |
| XI™ spectrometer | 0.12 | 5[a] |

[a]Assuming 60-min sample collection at 0.4 l min$^{-1}$.

## Laboratory evaluation

ESC test aerosols were used to assess the short-term measurement capability of the Raman method. Figure 4 shows a continuous measurement of number and mass concentration of a simulated transient RCS aerosol. The concentration of the QC test aerosol was intentionally varied periodically to mimic transient exposure over 200 min. The total aerosol mass concentration was monitored by the DustTrak™. Consecutive 20–30 min spot samples were collected for Raman analysis using the modified Nanozen™ cassette. This collection time was sufficient to measure RCS above LOQ of the Raman method. For comparison, filter samples were also collected for XRD analysis by the second co-located Nanozen™ monitor (using the standard cassette supplied by the manufacturer). However, larger collection time of 80–120 min was necessary to measure above LOD of the XRD method. The shaded region in Fig. 4 shows LOQ corresponding to 80 and

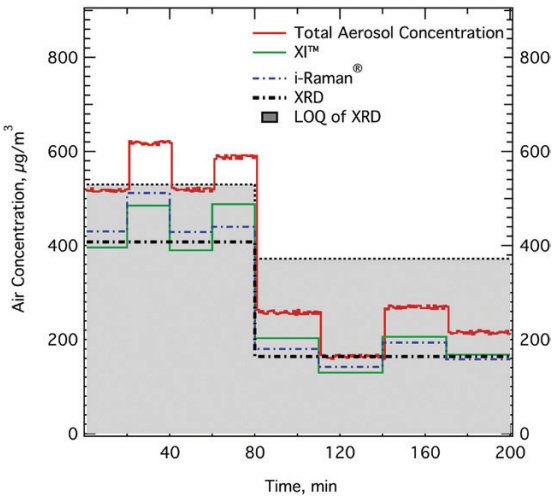


**Figure 4.** Short-term measurement of crystalline silica using the Raman method in a transient aerosol simulating work activity. The total aerosol concentration was maintained high to allow shorter collection times. Samples for both methods were collected using the Nanozen™ filter cassette. Minimum collection time of 20–30 min for the Raman method and 80–120 min for the XRD method was required to measure above LOQ. The shaded region shows the concentrations below LOQ of the XRD method; both XRD measurements were below LOQ. The average of four consecutive Raman measurements, over the first 80 min and thereafter, were within 10% of the XRD measurements over equivalent period.

120 min of collection time. As noted above, filter samples for Raman analysis were collected in succession during this time series measurement. In Fig. 4, the red curve shows the real-time total aerosol mass concentration air concentration measured by the DustTrak™. The blue and green curves show measured RCS concentration using XI™ and i-Raman® spectrometers, respectively. The orange curve shows the air concentration measured by XRD. The measured mass loadings and air concentrations using these two methods are shown in Table 3.

Due to different sample collection times of Raman and XRD methods, the air concentrations couldn't be directly compared across the two methods. The average concentration of 4 consecutive Raman measurements was 439.7 µg m$^{-3}$ from the XI™ and 452.7 µg m$^{-3}$ from i-Raman®; the RCS concentration measured using XRD over this 80 min period was 408 µg m$^{-3}$, about 7.7 and 9.9% lower compared to XI™ and i-Raman®, respectively. Similarly, the concentration over the next 120 min (between 80 and 200 min) was 164 µg m$^{-3}$ from the XRD measurements, which was lower by 7.2 and 2.7% compared to that measured by XI™ (176.7 µg m$^{-3}$) and i-Raman® (168.5 µg m$^{-3}$).

**Table 3.** Comparison of stone fabrication samples using Raman and XRD method.

| | Mass on filter, µg | | | RCS concentration, µg m$^{-3}$ | | |
|---|---|---|---|---|---|---|
| Cumulative time | i-Raman® | XI™ | XRD | i-Raman® | XI™ | XRD |
| 20 | 1.8 | 1.9 | 7.3[a] | 396 | 430 | 408 |
| 40 | 2.2 | 2.3 | | 485 | 512 | |
| 60 | 1.7 | 1.9 | | 390 | 429 | |
| 80 | 2.2 | 2.0 | | 488 | 440 | |
| 110 | 1.4 | 1.2 | 4.4[a] | 203 | 180 | 164 |
| 140 | 0.9 | 1.0 | | 130 | 142 | |
| 170 | 1.4 | 1.3 | | 206 | 194 | |
| 200 | 1.1 | 1.1 | | 168 | 158 | |

[a]Sample measured below LOQ of the XRD method.

## Field measurements

Table 4 shows the RCS concentration in personal breathing zone (PBZ) as well as in the workplace air (i.e. area samples) of various samples measured by the Raman and standard XRD methods. The number of personal and area samples that could be collected for method evaluation was limited due to resource constraints, as this study was conducted in conjunction with a separate exposure study at this worksite. This worksite has been well characterized in previous studies (Esswein *et al.*, 2013, 2018) for silica and diesel particulate matter (DPM) exposure. The sources of crystalline silica and DPM exposure in our study were very similar to those described by (Esswein *et al.*, 2013, 2018).

The total dust concentration ranged from 40 to 168 µg m$^{-3}$. The particulate elemental carbon (EC) and organic carbon (OC) content were measured in a separate exposure study conducted simultaneously. The EC and OC concentrations (determined using the NIOSH 5040 method) were found to vary widely in the exposure study. EC concentrations were in the range 1–85 µg m$^{-3}$. The OC concentrations were varied from 7 to 493 µg m$^{-3}$, with an average concentration of 40 µg m$^{-3}$ across all samples. These exposure measurements indicate that OC was a relatively significant portion of the silica-containing particulate matrix. The RCS fractional content, calculated as crystalline silica concentration divided by the total aerosol mass concentration, ranges from 3 to 30%.

Figure 5a,b show comparison of RCS concentration obtained from Raman (on y-axis) and the XRD (on x-axis) analysis. The linear regression curve (black line) and 95% confidence prediction interval around the best fit are also shown. Most data points are within the 95% confidence interval for both spectrometers; one data point for i-Raman® and three for XI™ are outside this

**Table 4.** Personal breathing zone (PBZ) and area exposure concentrations of RCS at a hydraulic fracturing worksite measured by Raman and XRD method.

| Sample/location | Sample type-number | Collection time (min) | RCS concentration, μg m$^{-3}$ | | | Total dust concentration, μg m$^{-3}$ | RCS content, % |
|---|---|---|---|---|---|---|---|
| | | | i-Raman® | XI™ | XRD | | |
| Line Boss | PBZ-1 | 580 | 5.5 | 5.5 | 5.3 | 65.6 | 8.1 |
| | PBZ-2 | 678 | 8.0 | 9.1 | 11.6 | 84.2 | 13.8 |
| | PBZ-3 | 685 | 3.3 | 3.9 | 3.5[a] | 90.0 | 3.9 |
| | PBZ-4 | 548 | 24.1 | 23.9 | 25.2 | 89.4 | 28.2 |
| Hydro-Acid Worker | PBZ-5 | 442 | 8.1 | 8.6 | 8.4 | 75.3 | 11.2 |
| | PBZ-6 | 675 | 27.6 | 29.1 | 32.4 | 168.5 | 19.2 |
| | PBZ-7 | 719 | 6.8 | 7.6 | 7.6 | 59.7 | 12.7 |
| Trailer Hitch | Area-1 | 146 | 5.3 | 4.9 | 4.3 | 50.7 | 8.5 |
| | Area-2 | 226 | 10.2 | 3.5 | 14.0 | 40.6 | 3.4 |
| Inside dance floor | Area-3 | 190 | 4.7 | 4.6 | 4.4 | 70.8 | 6.2 |
| Data Van | Area-4 | 190 | 3.0 | 3.2 | 2.9 | 74 | 4.0 |

[a]Sample measured below LOQ of the XRD method.

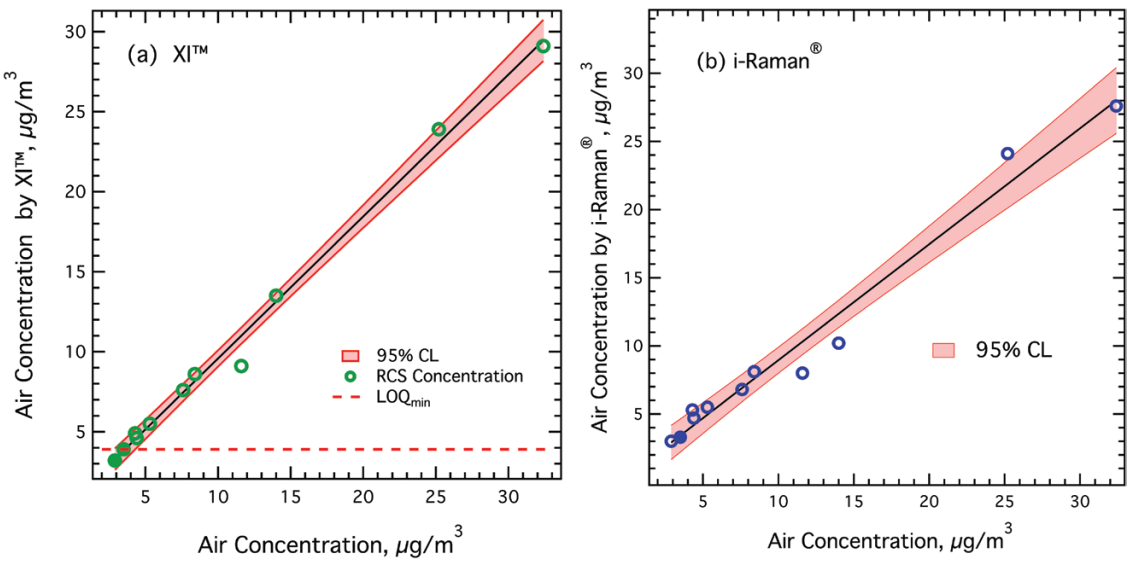


**Figure 5.** Comparison of crystalline silica concentration in workplace aerosol collected at a hydraulic fracturing site obtained using: (a) XI™ and (b) i-Raman® with the co-located XRD measurements. Samples for Raman analysis were collected using the Nanozen™ and those for the XRD method were collected using conventional filter cassettes. Filled symbols indicate samples measured below LOQ of the XRD method.

confidence interval. Overall, there appears to be a good agreement between the two methods. The coefficient of determination $R^2$ was 0.97.

The agreement is particularly good considering the difference in respirable size-selective inlets, sampling flow rates, and the calibration procedure between the two methods. The difference in calibration methods is particularly noteworthy. The Raman calibration curve was constructed using the particulate mass (of the aerosolized SRM) deduced from its air concentration measured in real-time by the DustTrak™ (which, in turn, was gravimetrically calibrated using the SRM). Since this is an optical sensing instrument, it does not provide a fundamental mass measurement, and therefore this estimation is not directly traceable to a NIST primary mass standard. In our study, the photometer was gravimetrically calibrated using the NIST SRM aerosol, which increased the accuracy of mass estimation. This approach, involving

aerosolized SRM, is preferable compared to the calibration using an aerosol with either unknown or a mixture of refractive indices. In contrast, the X-ray diffractometer measurement was calibrated using the spiked SRM aliquots and is therefore directly traceable to a NIST primary standard. Stacey *et al.* (2017) have also found a good agreement between the sensitivity of Raman measurements collected on filters and the sensitivity of measurement of aliquots of suspension pipetted onto filters.

Figure 6 shows results from Bland-Altman analysis (Bland and Altman, 1986) comparing the two methods for personal as well as area exposure concentrations. The y-axis in the plot shows the % relative difference ($\Delta$) in the concentrations from the two methods, defined as $\left(\frac{C_{Raman}-C_{XRD}}{C_{Raman}} \times 100\right)$, where $C_{XRD}$ and $C_{Raman}$ are concentrations from XRD and Raman methods. The x-axis shows the average concentration ($C_{mean}$) from the two methods, defined as $= \left(\frac{C_{XRD}+C_{Raman}}{2}\right)$. Also shown, in the plots are limits of agreement (LoA) (Bland and Altman, 1986) shown by the dotted lines around the $C_{mean}$, and defined as, $C_{mean} \pm 1.96\ \sigma_d$, where $\sigma_s$ is the standard deviation around $C_{mean}$. The shaded region around $\Delta$ shows 95% confidence interval. In case of perfect agreement between the two methods, $\Delta = 0$. The difference $\Delta$ ranges from 0.15% to –23.2%. The $\Delta = 0$ was within the confidence interval around $\Delta$, suggesting the difference between the methods may not be significant. All $\Delta$ values lie within the LoA, and majority of them lie inside the 95% confidence interval around $\Delta$. Values of $\Delta$ appears to be distributed randomly around $\Delta = 0$, though the number of samples is too small for meaningful conclusion. The agreement appears to be better for PBZ samples. The agreement between XI and XRD for one area sample (Area-2) was poor—it is not clear if this was a measurement artefact.

The magnitude of difference ($\Delta$) between the Raman and the XRD methods must be assessed in the context of intra- and inter-laboratory measurement precision associated with established XRD and infrared methods. For example, Stacey *et al.* (2003) have reported analytical precision for direct-on-filter methods of ±12% for XRD and ±14% for infrared techniques. They have also reported relative standard deviation (RSD) for variability of measurements within-laboratory using the indirect XRD method to be 6–34%. The relative difference ($\Delta$) in this study is comparable to uncertainties of the XRD method.

## Measurement considerations

Figure 7 shows the contour plots of minimum sample collection time needed to measure RCS above the LOQ of the Raman method using the Nanozen™ monitor. The minimum collection time was calculated as follows:

$$t_{min} = m_{loq}/(C_{total} \times \omega_{RCS} \times Q) \qquad (2)$$

where $t_{min}$is the minimum sample collection time required to measure above $m_{loq}$; $Q$ is the sampling flow rate of the Nanozen™ dust monitor; $c_{total}$ is the air concentration of airborne dust; and $\omega_{RCS}$ is the fractional content of RCS in total dust.

In Fig.7a, the minimum collection time of XI™ is 8 min while in Fig.7b the minimum collection time of i-Raman® is 30 min. Also, for the XRD method, it will take more than 4 hours to measure above LOQ, if the air concentration is lower than 20 μg m$^{-3}$, even for pure RCS samples. Figure 7 is useful for guiding sample collection in the field when approximate % RCS is known *a priori*. For example, if a given workplace, the total aerosol mass concentration and RCS fraction are expected to be about 200 μg m$^{-3}$ and 20%, then a minimum collection time of 23 min and 95 min may be

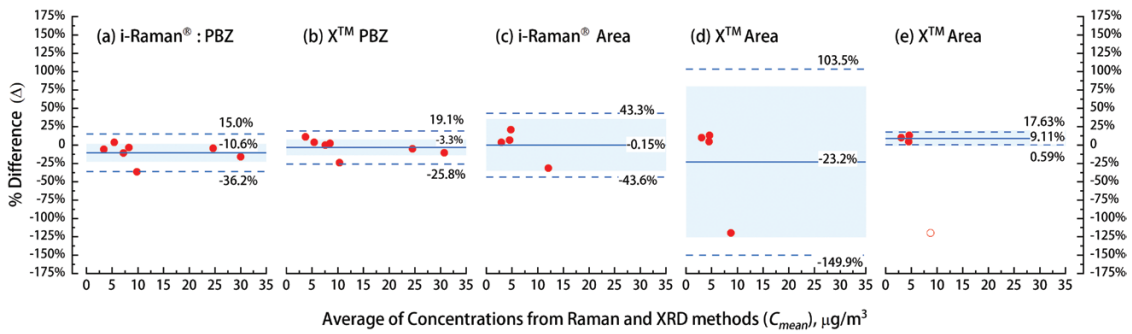


**Figure 6.** Bland-Altman plots showing comparison of Raman and XRD methods for area and PBZ samples. Distribution of $\Delta$ as a function of *Cmean* for PBZ samples (a) by i-Raman and (b) XI, and area samples (c) by i-Raman, (d) XI including an outlier sample, and (e) XI excluding an outlier sample (shown by open symbol).

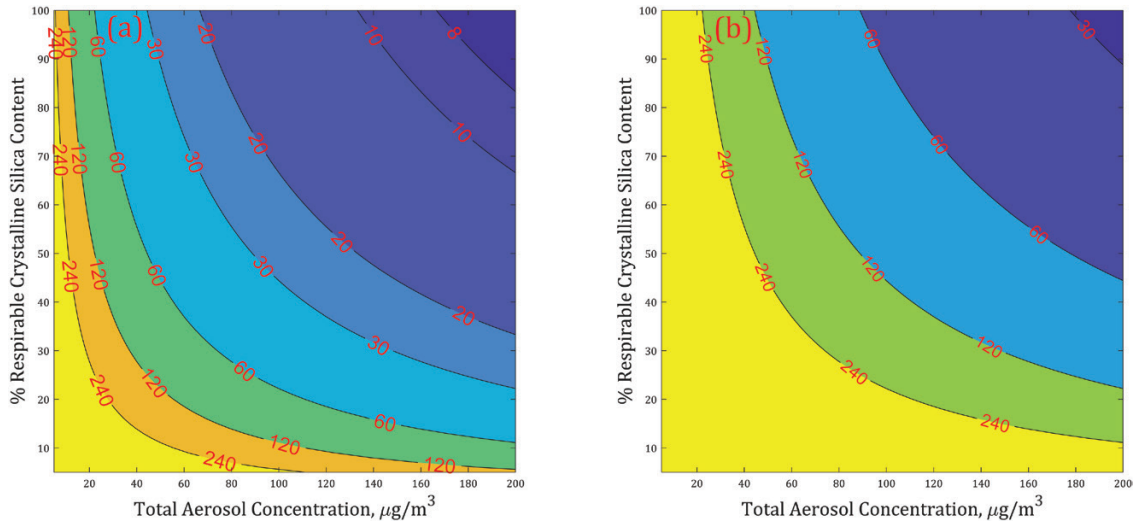


**Figure 7.** Contour maps of minimum sample collection times, in minutes (contour labels in red), required to measure RCS above limit of quantification of (a) XI™ and (b) i-Raman® for a range of total aerosol concentrations and corresponding fractional contents of RCS (in percent). These maps can be used to estimate the approximate collection time needed using the Nanozen™ dust monitor, if approximate range of total dust concentration and fractional silica content are known.

appropriate to measure above the LOQ for XI™ and i-Raman®, respectively.

Though the focus in this study was on measurement of an α-quartz, the Raman method can also measure other polymorphs of crystalline silica including cristobalite (610 or 230 $cm^{-1}$) and tridymite (356 $cm^{-1}$) with a spectrometer that has good (< 4 $cm^{-1}$) wavenumber resolution (Zheng *et al.*, 2018). Good agreement between the Raman and the XRD methods for both field and laboratory measurements suggest that the approach could provide onsite, direct-on-filter measurement of RCS using commercially available aerosol monitors and Raman spectrometers for aerosols studied in this work. However, performance of the method can strongly depend on the matrix interferents, and other artefacts discussed below, which will need to be further investigated. Both, the handheld and portable approaches are particularly useful for making quick, on-site measurement of short-term exposures that are not possible using the XRD method. As discussed earlier, for a given spectrometer configuration, spot sample collection is necessary to achieve low detection limits; however, it may not be necessary if higher detection limits or full-shift collection are adequate. For instance, we estimate based on this and our previous study (Zheng *et al.*, 2018), that 8-h collection at 1 l $min^{-1}$ over a 10-mm diameter filter may still allow measuring at sufficiently low LOQ in the range 15–25 μg $m^{-3}$. Such wide-area collection may allow using conventional samplers and filter cassettes routinely used in workplace air monitoring that don't require spot sample as small as 1.5 mm diameter.

While the direct-on-filter Raman method has advantages with respect to speed and ease of analysis, it is prone to spectral or matrix interferences that may diminish the analytical figures of merit for some workplace aerosol samples. These interfering species could be components in the workplace aerosols or from outdoor atmospheric aerosols. As discussed elsewhere (Zheng *et al.*, 2018), interference from secondary organics, nitrates, and particulate carbon in ambient aerosols is less likely. However, sulfates present in atmospheric aerosols show a peak at ~450 $cm^{-1}$ and may potentially interfere, particularly if the spectrometer's wavenumber resolution is poor or if the sulfates are present in large quantities relative to crystalline silica (urban ambient sulfate concentration are typically ~0.3–40 μg $m^{-3}$ in the USA (Weber *et al.*, 2003)). Interference from other inorganic mineral constituents in the particulate phase could also affect the measurement of α-quartz. Cristobalite, tridymite, kaolinite, and other minerals have Raman peaks with varying degree of overlap with that of α-quartz and could interfere if present in high relative concentrations (Zheng *et al.*, 2018). Peak deconvolution and fitting or correction schemes involving non-overlapping peaks of interferents (for example as is done in infrared methods to account for kaolinite interference) may allow correcting for such interferences in some cases. Stacey *et al.* (2017, 2020) have reported interference from photon absorbing components such as hematite or metallic components, which can also introduce bias.

Sample fluorescence is another artefact that affects all Raman measurements. Some workplace aerosols

containing large organic or biogenic fractions could lead to increased fluorescence during acquisition of Raman spectra, which may further deteriorate the detection limits. Also, some samples, particularly those containing large carbonaceous fraction or metal oxides, may cause localized heating and become thermally unstable during the Raman measurement. Our recent work on carbonaceous aerosols shows that such thermal effects could be minimized by using a conducting substrate, such as the silver membrane filter used in this study (Zheng and Kulkarni, 2019). Our experience with several types of workplace aerosols from construction and hydraulic fracturing industries (Zheng and Kulkarni, 2019) including those described in this work, shows that meaningful Raman measurements can be performed without interference from fluorescence and thermal effects.

Variation in ambient humidity or moisture content of filter, especially between calibration and field sample measurements, can also affect the RCS quantification. Higher humidity can lead to elevated baseline of Raman spectrum, which in turn, may affect either sensitivity or dynamic range of the measurement. Our experience shows that dry filter samples produce reproducible and low-baseline spectra. Using temperature-controlled filter sample accessory will significantly increase reproducibility and sensitivity of measurements.

When extending this method to workplace atmospheres, where very little is known about potential interferents, expected range of RCS concentration, or the approximate fractional silica content, significant caution must be exercised to assess the effect of sample fluorescence, sample stability, and matrix or spectral interference. Further studies in various occupational environments will be necessary to assess the broader applicability of the method.

The study shows that the approach, involving combination of real-time wearable particulate monitor and on-site Raman measurement, has the potential for broader adoption as an on-site or in-field method by non-expert professionals (those not trained in Raman spectroscopy). The approach is also cost-effective, allowing users to collect short-term samples if needed or collect large a number of samples. Judicious use of the approach can also allow designing effective silica exposure monitoring program and can help reduce the number of compliance samples and the analysis costs thereof. If the measurement uncertainties are unacceptably high for a certain particle matrix, the method can still provide semi-quantitative or qualitative measurements quickly onsite, which can be useful in some applications such as assessment of engineering controls.

However, further development of standardized hardware accessories and software add-ons will be necessary to simplify the measurements and minimize the artefacts. Many Raman instrumentation manufacturers sell application-specific probes, cells, and accessories for interfacing with samples for a broad range of industrial measurements in pharmaceutical, manufacturing, environmental monitoring, and process industries. Similar, accessories can be developed for filter sample analysis that allow quick and easy direct-on-filter analysis with different Raman spectrometers. Software add-ons will need to be developed to allow user-friendly instrument control and display of analyte air concentration. The approach can possibly be extended to other workplace aerosols such as diesel particulate matter and nanomaterials that have unique Raman signatures.

## Conclusions

A direct-on-filter approach for on-site measurement of crystalline silica concentration in workplace atmospheres was described. The modified filter cassette that achieves 1.5-mm-diameter spot sample provides adequate tradeoffs between time resolution, detection limits, and pressure drop. Calibration of the method using aerosolized SRM yielded mass detection limits about an order of magnitude lower than those for the current standard XRD method. The lowest limit of quantification for α-quartz was 16.6 μg $m^{-3}$ at a sample collection time of 1 h using the handheld Raman spectrometer, which was significantly below that for the standard XRD method (67.5 μg $m^{-3}$ at 4.2 l $min^{-1}$ and 1 h collection). The direct-on-filter method may also allow full-shift (8-h) measurements below the action levels of 25 μg $m^{-3}$ or lower, using convention filter cassette collection commonly used in industrial hygiene measurements.

Field measurements at a hydraulic fracturing site showed good agreement between co-located Raman and XRD measurements, though the number of field samples was too small to draw broad conclusions. The pilot study demonstrates the potential of handheld Raman spectrometers to provide quantification with analytical figures of merit comparable to the standard XRD analytical method for the silica-containing aerosols studied in this work.

The direct-on-filter nature of analysis (and the lack of sample preparation) also requires caution in evaluating or minimizing measurement artefacts typical in Raman analysis. Standardizing hardware accessories for filter sample analysis will go a long way in reducing such artefacts. Though the laboratory and field measurements in this study were not met with such limitations, further

extensive field studies will be required to probe matrix interferences, measurement artefacts, and the associated uncertainties. This will allow assessment of broader applicability of the Raman method for RCS analysis in various occupational and industrial environments.

The direct-on-filter Raman method can be a valuable tool for reducing cost of routine RCS exposure measurements or compliance-related monitoring. Judicious use of this approach, in conjunction with standard analytical or compliance methods, can potentially improve the efficacy of crystalline silica exposure monitoring and control in many occupational environments.

## Supplementary Data

Supplementary data are available at *Annals of Work Exposures and Health* online.

## Acknowledgements

The authors are grateful to Dr. Lynn Chandler of CloudMinds Inc. for loaning the Raman instrument for this study. The authors also thank Dr. Winnie Chu and Peter Briscoe of Nanozen Industries Inc. for providing the drawings of Nanozen™ filter cassette. The authors are grateful to Dr. Peter Stacey of UK HSE for providing thoughtful feedback on this work. The work was supported by intramural grant from the National Institute for Occupational Safety and Health, grant (CAN 939051U). The findings and conclusions in this report are those of the authors and do not necessarily represent the official position of the National Institute for Occupational Safety and Health. Mention of product or company name does not constitute endorsement by the Centers for Disease Control and Prevention.

## Conflict of interest

The authors declare no conflict of interest relating to the material presented in this article. Its contents, including any opinions and/or conclusions expressed, are solely those of the authors.

## Data availability

The data underlying this article are available in the article and in its Supplementary Material.

## References

ACGIH. (2006) *Threshold limit values (TLVs) and biological exposure indices (BEIs)*. Cincinnati, OH: American Conference of Governmental Industrial Hygienists.

Akbar-Khanzadeh F, Brillhart RL. (2002) Respirable crystalline silica dust exposure during concrete finishing (grinding) using hand-held grinders in the construction industry. *Ann Occup Hyg*; **46**: 341–6.

Baron PA, Rice FL, Key-Schwartz R, Bartley D, Schlecht P. (2002) *Health effects of occupational exposure to respirable crystalline silica*. NIOSH hazard review; DHHS (NIOSH) Publication No 2002–129. https://www.cdc.gov/niosh/docs/2002129/pdfs/2002129.pdf?id=10.26616/NIOSHPUB2002129.

Bland JM, Altman DG. (1986) Statistical methods for assessing agreement between two methods of clinical measurement. *Lancet*; **1**: 307–10.

Boumans PWJM. (1994) Detection limits. *Anal Chem*; **66**: 459A–67A.

Chen BT, Fletcher RA, Cheng YS. (2011) Calibration of aerosol instruments. In: Kulkarni P, Baron AP, Willeke K, editors. *Aerosol measurement: principles, techniques, and applications*. 3rd edn. Hoboken, NJ: John Wiley & Sons Inc. pp. 449–78.

Chisholm J. (1999) Respirable dust and respirable silica concentrations from construction activities. *Indoor Built Environ*; **8**: 94–106.

Esswein EJ, Alexander-Scott M, Snawder J *et al*. (2018) Measurement of area and personal breathing zone concentrations of diesel particulate matter (DPM) during oil and gas extraction operations, including hydraulic fracturing. *J Occup Environ Hyg*; **15**: 63–70.

Esswein EJ, Breitenstein M, Snawder J *et al*. (2013) Occupational exposures to respirable crystalline silica during hydraulic fracturing. *J Occup Environ Hyg*; **10**: 347–56.

IARC. (1997) *Silica, some silicates, coal dust and Para-aramid fibrils. IARC Monographs on the Evaluation of Carcinogenic Risks to Humans*. No. 68. Lyon, FR: International Agency for Research on Cancer.

IARC. (2012) *Silica dust, crystalline, in the form of quartz or cristobalite. IARC Monographs on the Evaluation of Carcinogenic Risks to Humans*. No. 100C. Lyon, FR: International Agency for Research on Cancer.

Kingma KJ, Hemley RJ. (1994) Raman spectroscopic study of microcrystalline silica. *Am Mineral*; **79**: 269–73.

Linch KD. (2002) Respirable concrete dust–silicosis hazard in the construction industry. *Appl Occup Environ Hyg*; **17**: 209–21.

Meeker JD, Cooper MR, Lefkowitz D *et al*. (2009) Engineering control technologies to reduce occupational silica exposures in masonry cutting and tuckpointing. *Public Health Rep*; **124** (Suppl. 1): 101–11.

Mu T, Li S, Feng H, Zhang C, Wang B, Ma X, Guo J, Huang B, Zhu L. (2019) High-sensitive smartphone-based raman system based on cloud network architecture. *IEEE J Select Top Quantum Electron*; **25**: 1–6.

NIOSH. (1987) *Occupational respiratory diseases*. National Institute for Occupational Safety and Health (NIOSH). DHHS (NIOSH) Publication No 86–102. https://www.cdc.gov/niosh/docs/86102/86102.pdf?id=10.26616/NIOSHPUB86102.

NIOSH. (1994) Particulates not otherwise regulated, total; NIOSH Method 0500. In NIOSH editor. *NIOSH Manual of Analytical Methods (NMAM)*, Fourth Edition. Cincinnati, OH: U.S. Department of Health and Human Services.

NIOSH. (2003) *SILICA, CRYSTALLINE, by XRD (filter redeposition): METHOD 7500*. https://www.cdc.gov/niosh/docs/2003154/pdfs/7500.pdf.

NIOSH. (2017) *QUARTZ in respirable coal mine dust, by IR (redeposition): METHOD 7603*. NIOSH Manual of Analytical Methods (NMAM), 5th edn. https://www.cdc.gov/niosh/nmam/pdf/7603.pdf.

OSHA. (2016) Occupational exposure to respirable crystalline silica; final rule. *Fed. Regist.* **81**: 16285–890. https://pubmed.ncbi.nlm.nih.gov/27017634/.

Qi C, Echt A. (2019) *Field evaluation of a mobile dust control booth for stone countertop grinding*. National Institute of Occupational Safety and Health, Internal Report, EPHB Report No. 2020-DFSE-165. https://www.cdc.gov/niosh/surveyreports/pdfs/2020-DFSE-165.pdf. Accessed September 23, 2021.

Rappaport SM, Goldberg M, Susi P *et al*. (2003) Excessive exposure to silica in the US construction industry. *Ann Occup Hyg*; **47**: 111–22.

Stacey P, Clegg F, Morton J *et al*. (2020) An indirect Raman spectroscopy method for the quantitative measurement of respirable crystalline silica collected on filters inside respiratory equipment. *Anal Methods*; **12**: 2757–71.

Stacey P, Mader KT, Sammon C. (2017) Feasibility of the quantification of respirable crystalline silica by mass on aerosol sampling filters using Raman microscopy. *J Raman Spec*; **48**: 720–25.

Stacey P, Tylee B, Bard D, Atkinson R. (2003) The performance of laboratories analysing α-Quartz in the Workplace Analysis Scheme for Proficiency (WASP). *Ann occup Hyg*; **47**: 269–77. doi:10.1093/annhyg/meg026.

Weber R, Orsini D, Duan Y, *et al*. (2003) Intercomparison of near real time monitors of PM2.5 nitrate and sulfate at the U.S. Environmental Protection Agency Atlanta Supersite. *J Geophys Res Atmos*; **108**: 8421.

Wei S, Kulkarni P, Ashley K *et al*. (2017) Measurement of crystalline silica aerosol using quantum cascade laser-based infrared spectroscopy. *Sci Rep*; **7**: 13860.

Wei S, Kulkarni P, Zheng L, Ashley K. (2020) Aerosol analysis using quantum cascade laser infrared spectroscopy: application to crystalline silica measurement. *J Aerosol Sci*; **150**: 105643.

Yassin A, Yebesi F, Tingle R. (2005) Occupational exposure to crystalline silica dust in the United States, 1988–2003. *Environ Health Perspect*; **113**: 255–60.

Zheng L, Kulkarni P. (2019) Real-time measurement of airborne carbon nanotubes in workplace atmospheres. *Anal Chem*; **91**: 12713–23.

Zheng L, Kulkarni P, Birch ME *et al*. (2018) Analysis of crystalline silica aerosol using portable Raman spectrometry: feasibility of near real-time measurement. *Anal Chem*; **90**: 6229–39.